Even-parity states of the Sm atom with stepwise excitation*

Li Ming(李 鸣)[a)b)], Dai Chang-Jian(戴长建)[a)b)†], and Xie Jun(谢 军)[a)b)]

[a)] *Key Laboratory of Display Materials and Photoelectric Devices of Ministry of Education, Tianjin* 300384, *China*

[b)] *School of Science, Tianjin University of Technology, Tianjin* 300384, *China*

(Received 25 February 2010; revised manuscript received 20 January 2011)

Two-colour stepwise excitation and photoionization schemes are adopted to study the spectra of high-lying states of the Sm atom. These bound even-parity states are excited with three different excitation paths from the $4f^6 6s6p\,^7D_J$ (J = 1, 2, 3) intermediate states, respectively. They are probed by photoionization process with an extra photon driving them to the continuum states. In this experiment, 270 states are detected in an energy range from 36160 cm^{-1} to 42250 cm^{-1}, 109 of which are newly discovered, while the rest of them are confirmed to be the energy levels reported previously. Furthermore, based on the J-momentum selection rules of three excitation paths, a unique assignment of J-momentum for all observed states is determined, eliminating all remaining ambiguities in the literature. Finally, 53 single-colour transitions originating from the scanning laser are also identified. For all the relevant transitions, the information about their relative intensities is also given in the paper.

Keywords: stepwise excitation, Sm atom, even-parity, high-lying states

PACS: 32.80.Fb, 32.30.Jc, 32.70.FW **DOI:** 10.1088/1674-1056/20/6/063204

1. Introduction

Since the advent of tunable lasers, many studies on high-lying states of atoms have been carried out.[1−4] To explore their bound Rydberg states and autoionizing Rydberg states, the technique of stepwise excitation has been used extensively.[5−7] Compared with single-step excitation, the stepwise excitation technique has several advantages:[8] first, each step drives a resonant transition where only low laser intensity is required; secondly, many different final states can be excited by selecting different excitation schemes. With this method, alkaline-earth atoms, such as Ba,[9,10] Mg,[11,12] and Sr,[13,14] have been systematically studied. These efforts lead to not only the accumulation of a great many atomic data, but also the enhancement of our knowledge in some relevant fields. For instance, the coupling effect of electron–electron or electron–ion manifested in autoionization states has profoundly promoted our understanding of mechanism for the dielectronic recombination process.[15]

On the contrary, the study of high-lying states of rare-earth atoms is scanty,[16−18] which is due mainly to the fact that these elements have an unfilled 4f subshell, leading to very complex atomic spectra. The only exception is the Yb atom, which has been studied most[19,20] as it has a completely filled 4f shell. Since there are six electrons in the 4f sub-shell[21] for the Sm atom, its spectra are formed by two kinds of electron transitions: a) the outer $6s^2$ electrons; b) those in the inner unstable $4f^6$ shell. In addition, the seven fine structures of the ground state of Sm atom, $4f^6 6s^2(^7F_J)$ (J = 0, 1, 2, ..., 6), are readily populated thermally during heating the Sm metal to obtain the atomic beam.[22] The above complex features make the study on Sm atom very difficult,[23,24] so the existing papers deal mainly with the odd-parity excited states with one tunable laser.[23,25] With all the facts in mind, in this work we will concern the spectra of high-lying even-parity states of Sm atom, systematically study the excitations from three different intermediate states having the same electron configuration.

In the following text, an experimental setup will be presented in Section 2; experimental results and discussion will be given in Section 3; and several conclusions will be presented in Section 4.

*Project supported by the National Natural Science Foundation of China (Grant Nos. 10574098 and 10674102) and the Natural Science Foundation of Tianjin, China (Grant No. 05YFJMJC05200).

†Corresponding author. E-mail: daicj@126.com

© 2011 Chinese Physical Society and IOP Publishing Ltd

2. Experiment

The experimental setup and approach used here were described in detail elsewhere,[22] so only some relevant features will be illustrated in this paper. As shown in Fig. 1, the experimental setup is comprised of three parts, i.e., a laser system, an atomic beam system and a data acquisition system.

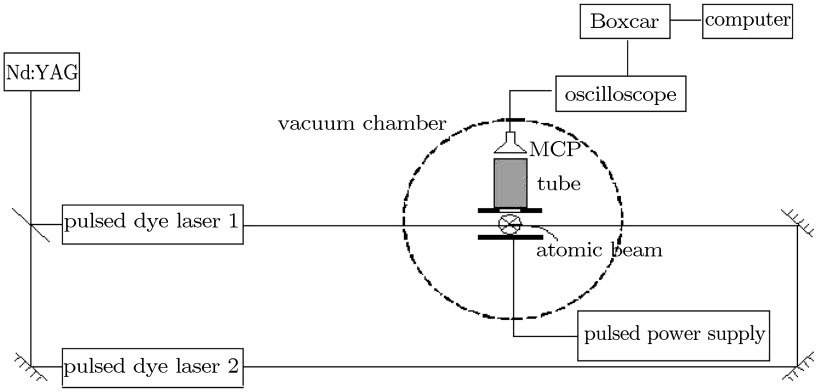


Fig. 1. Schematic diagram of the experimental setup. It includes a laser system, an atomic beam system and a data acquisition system. The atomic beam interacts with three laser beams in the vacuum chamber. The ion signal is detected by an MCP, integrated and averaged by a Boxcar and stored in a computer for further analysis.

Specifically, the laser system consists of two tunable dye lasers pumped by the same Nd:YAG pulsed laser with a wavelength of 532 nm or 355 nm, corresponding to the second or the third harmonics generation (SHG or THG) of Nd:YAG laser. In order to ensure that the two laser pulses are sequential in time, the pulse of the second dye laser has a 10-ns delay relative to the pulse of the first dye laser. Typically, the dye laser has an 8-ns pulse duration, a 0.1-cm^{-1} line width and a 0.5-mJ pulse energy. The atomic beam system is composed of an atomic oven, a DC power supply, a temperature controller and a collimator. The oven is resistively heated and typically maintained at 800 K. To avoid the Doppler broadening, the atomic beam is crossed perpendicularly by the two laser beams in a region between two electric field plates with 1-cm separation. About 500 ns after the laser pulses, a 50-V electric pulse is applied to the plates, sweeping the Sm ions resulting from photoionization process into an MCP detector through a grid on one of the plates. The data acquisition system consists of a Boxcar integrator, digital pulse generator and computer system. The ion signal detected by the MCP is integrated and averaged by the Boxcar whose output is digitized with an ADC and stored in a computer for further analysis.

In order to ensure the accuracy of experimental data, the possible experimental errors need to be reduced. For instance, the wavelength of the dye laser is absolutely calibrated with the optogalvanic spectra of hollows-cathode lamps, whose spectral lines are known accurately and is relatively calibrated by the spectrum of a Fabry–Perot etalon, which can correct the nonlinearity in each scan. In addition, each spectrum is measured several times, of which the average may reduce the statistical errors. With all efforts mentioned above, the present work can provide the level energies with an accuracy better than ± 0.1 cm^{-1}.

Turning now to the excitation schemes used in the experiment, the relevant energy levels are illustrated in Fig. 2. As shown in Fig. 2(a), the Sm atom can be excited to three intermediate states $4f^6 6s6p(^7D_J)$, where $J = 1$, 2, and 3, by first laser λ_1. The photon with varied wavelength of λ_2 excites Sm atom further to many bound even-parity states, where it is probed by photoionization process by driving it to the continuum states with an extra λ_2 photon.

It is well known that the ground state of the Sm atom has seven fine structures, $4f^6 6s^2(^7F_J)$ $(J = 0, 1, 2, \ldots, 6)$,[26,27] of which the thermal populations at 800 K are 21.03%($^7F_0$), 37.83%($^7F_1$), 25.45%($^7F_2$), 10.98%($^7F_3$), 5.55%($^7F_4$), 0.99%($^7F_5$), and 0.25%($^7F_6$).[22] In order to design an efficient excitation scheme, one needs to select a state from the above seven states as an initial state and choose a state from many candidates, due to the selection rules, as an intermediate state of the transitions as shown in Fig. 2(a). Obviously, to make such a selection, both factors, population percentage of the initial state and transition probability of the first-step ex-

citation, must be considered simultaneously. In the experiment, the overall intensity of about 20 possible transitions from the initial states to the intermediate states are carefully evaluated by comparing their ionization signals with a UV photon at 355 nm from the THG of the YAG laser. The initial state and intermediate state are selected by picking up the transition with the strongest ionization signal. With this method, two initial states and three intermediate states are determined. If the $4f^6 6s^2(^7F_1)$ state, with the most thermal population, is chosen as the initial state, then the $4f^6 6s6p(^7D_J)$ (J = 1, 2) states are chosen as the intermediate states. However, the signal from the $4f^6 6s^2(^7F_3)$ initial state to the $4f^6 6s6p(^7D_3)$ state is found to be strongest, although the thermal population of $4f^6 6s^2(^7F_3)$ state is less than that of $4f^6 6s^2(^7F_2)$ state.

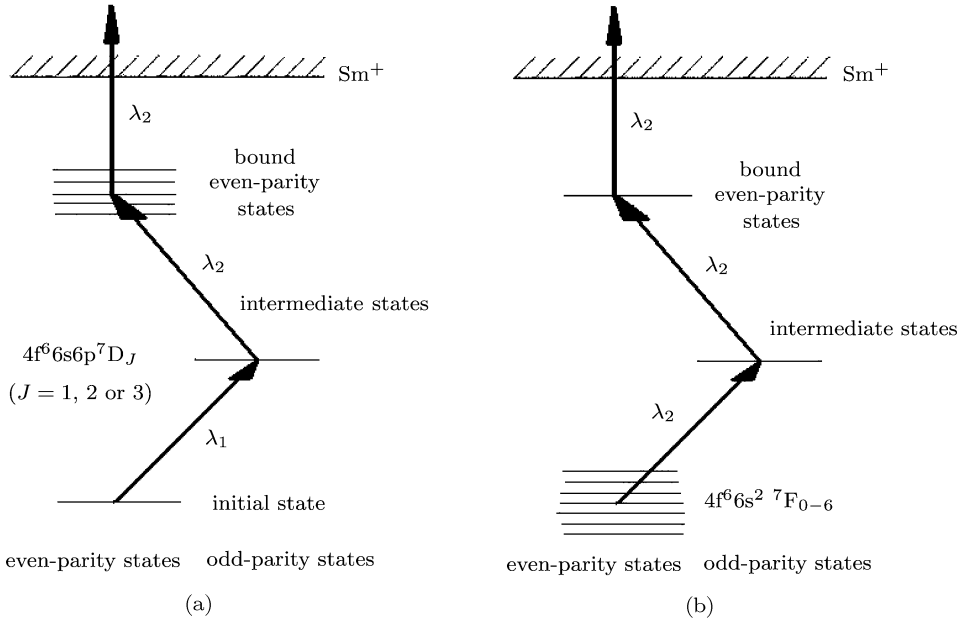


Fig. 2. Excitation schemes used in the experiment: (a) two-colour stepwise $\lambda_1+\lambda_2+\lambda_2$ process; (b) single-colour stepwise $\lambda_2+\lambda_2+\lambda_2$ process.

As mentioned above, adopted in the present work are two initial states, $4f^6 6s^2(^7F_J)$ (J = 1, 3), and three intermediate states, $4f^6 6s6p$ (^7D_J) (J = 1, 2, 3), for the study of bound even-parity states. Namely, the Sm atom is excited to the even-parity states with two pulsed dye lasers via the following three paths:

(I) $4f^6 6s^2(^7F_1) \xrightarrow{\lambda_1=478.444\ \text{nm}} 4f^6 6s6p\ (^7D_1) \xrightarrow{\lambda_2} E_J\ (J = 0, 1, 2) \xrightarrow{\lambda_2} Sm^+$,
(II) $4f^6 6s^2(^7F_1) \xrightarrow{\lambda_1=464.670\ \text{nm}} 4f^6 6s6p\ (^7D_2) \xrightarrow{\lambda_2} E_J\ (J = 1, 2, 3) \xrightarrow{\lambda_2} Sm^+$,
(III) $4f^6 6s^2(^7F_3) \xrightarrow{\lambda_1=472.975\ \text{nm}} 4f^6 6s6p\ (^7D_3) \xrightarrow{\lambda_2} E_J\ (J = 2, 3, 4) \xrightarrow{\lambda_2} Sm^+$.

The possible values of total angular momentum of the final states are given. In path I, the first laser with a wavelength of 478.444 nm excites the Sm atom from the initial state $4f^6 6s^2(^7F_1)$ at 292.58 cm^{-1} to the odd-parity $4f^6 6s6p(^7D_2)$ state at 21193.68 cm^{-1} and then the second laser with scanned wavelength excites it further to the bound even-parity states. In path II, the first laser with a wavelength of 464.670 nm excites the Sm atom from the $4f^6 6s^2(^7F_1)$ state to the odd-parity $4f^6 6s6p(^7D_2)$ state at 21813.22 cm^{-1} and then the second laser with scanned wavelength excites it further to the bound even-parity states. Similarly, in path III, the $4f^6 6s6p(^7D_3)$ state at 22633.30 cm^{-1} is populated by the first laser whose wavelength is fixed at 472.975 nm, from the initial state $4f^6 6s^2(^7F_3)$ at 1489.55 cm^{-1} and then the second laser excites it further to the bound even-parity states.[28]

In addition to the level energy E of the even-parity states, the total angular momentum J can also be assigned unambiguously to them. To be exact, the J value of every peak can be determined by comparing the spectra obtained from the three paths, as their selection rules of dipole transitions yield the different possible values. Specifically, in path I, the possible

values of total angular momentum of the bound state are $J = 0$, 1 or 2, while $J = 1$, 2 or 3 and $J = 2$, 3 or 4 for the paths II and III, respectively. Thus, the detailed comparisons mentioned above enable us to assign the value of J for each peak appearing in any of observed spectra, which have the five possible cases as shown in Table 1.

In case 2, for instance, if a peak is present in the two spectra with the paths I and II, respectively, but it is absent in the one with the path III, then $J = 1$ can be assigned to it. Similarly, the J values for other four different cases may also be determined from Table 1.

Table 1. The J values for five different cases. Each case represents the specific result of comparison for the same peak obtained with the three different paths.

Case	Path I	Path II	Path III	J
1	present	absent	absent	0
2	present	present	absent	1
3	present	present	present	2
4	absent	present	present	3
5	absent	absent	present	4

On the other hand, in order to get rid of accidental signals from two-photon or three-photon transitions, the light intensities of both lasers are monitored carefully during the experiment. Besides, it is found that signals from some multistep single-colour resonance transitions may also disturb the desired $\lambda_1 + \lambda_2 + \lambda_2$ process.

For instance, the ionization signals from λ_2 alone can be identified as $\lambda_2 + \lambda_2 + \lambda_2$ process as shown in Fig. 2(b).[22] Therefore, in order to discriminate the unexpected signals, it is necessary to make comparisons between two cases where spectra are obtained with and without the λ_1 photon, while λ_2 is scanned within the same region. Based on the above comparison, it is easy to indicate which peak belongs to the multistep single-colour process. Thus, the energy of a bound even-parity state probed by the $\lambda_1 + \lambda_2 + \lambda_2$ process can be determined by adding the photon energies of λ_1 and λ_2. Note that all wavelengths used in this work are the values in vacuum.

3. Results and discussion

With the principles shown in Table 1, we are able to analyse the spectra obtained with different excitation paths. A typical comparison of two-colour stepwise photoionization spectra of the Sm atom in the lower energy region between 37300 cm^{-1} and 37550 cm^{-1} is shown in Fig. 3, where the abscissa is the sum of photon energies of λ_1 and λ_2.

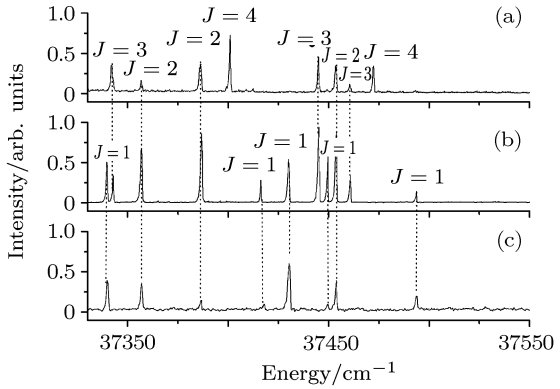


Fig. 3. Photoionization spectra of even-parity high-lying states in the lower energy region: (a) with path I, (b) with path II, and (c) with path III. The J values are assigned to many peaks and the abscissa represents the term energy.

As shown in Fig. 3, the total angular momentum J can be unambiguously assigned to each peak. Taking the one on the far left-hand side of Fig. 3 for instance, it is present in the two spectra obtained with the paths I and II, but is absent from that with the path III. Therefore, the comparisons enable us to assign it to a unique value of $J = 1$, which is the state of No. 73 shown in Table 3.

Similarly, figure 4 displays another example of comparisons in the higher energy region between 41740 cm^{-1} and 42250 cm^{-1}. In Fig. 4, the peaks marked with the numbers 0, 1, 2, 3, and 4 indicate that they can uniquely assigned with $J = 0$, 1, 2, 3, and 4, respectively.

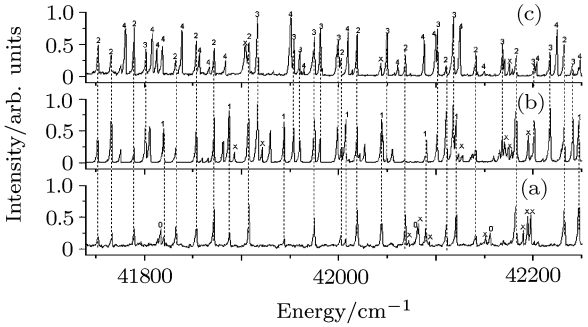


Fig. 4. Photoionization spectra of even-parity high-lying states in the higher energy region: (a) with path I, (b) with path II, and (c) with path III. The J values are assigned to many peaks and the abscissa represents term energy.

As shown in Fig. 4, there are a lot of unexpected peaks, marked with "×" sign. Since they originate from the $\lambda_2 + \lambda_2 + \lambda_2$ photoionization process, as described in Section 2, we may discriminate them by

blocking the first laser during the experiment. Meanwhile, it is evident that the density of state in the higher energy region becomes much higher than that in the lower energy region as expected.

With the same procedures as those used in Figs. 3 and 4, all the experimental spectra are analysed, from which the spectroscopic information about 270 even-parity states, including their level energy E, line intensity I and unique assignment of J value, is shown in Tables 2 and 3. In addition, in order to make different transitions comparable, their relative intensities are normalized to one and the letters w (weak), m (medium) and s (strong) are used to represent the intensities from 0 to 0.3, from 0.4 to 0.6 and from 0.7 to 1, respectively.

Now let us pay our attention to the spectroscopic information shown in Table 2. Although the level energies of these 79 states have previously been reported with different methods, they failed to provide a unique J-assignment and the line intensity for them.[26,30]

Table 2. Level energy E values of Sm even-parity states, to be compared with those in Refs. [26] and [30]. The extra information about relative intensities I and the unique J assignment is also given.

Serial number	E/cm^{-1}	J	I	Serial number	E/cm^{-1}	J	I
1	42247.17	2	m	41	40003.77	4	w
2	42240.81	3	m	42	39986.91	4	w
3	42224.01	4	s	43	39908.75	4	w
4	42217.22	3	s	44	39666.54	4	m
5	42203.64	4	m	45	39634.26	4	m
6	42182.30	3	s	46	39609.17	4	m
7	42140.84	2	m	47	39566.95	4	w
8	42120.57	1	m	48	39548.05	1	w
9	42117.80	3	s	49	39535.52	4	s
10	42110.81	1	s	50	39408.34	3	m
11	42101.12	3	m	51	39245.81	1	m
12	42099.10	4	m	52	39243.11	2	s
13	42068.46	2	s	53	39178.71	2	m
14	42049.41	3	m	54	38916.40	3	s
15	42043.98	1	m	55	38860.19	1	w
16	42006.98	1	s	56	38793.25	3	m
17	42002.38	2	m	57	38700.09	2	s
18	41980.92	3	m	58	38596.08	4	w
19	41974.72	3	s	59	38184.43	3	m
20	41959.63	2	s	60	38089.61	4	m
21	41953.57	3	s	61	38065.55	4	m
22	41950.29	4	m	62	38033.79	4	s
23	41943.77	1	s	63	37932.54	4	m
24	41871.53	2	s	64	37449.46	2	s
25	41853.20	1	s	65	37356.81	2	s
26	41838.21	4	w	66	37174.69	2	s
27	41832.25	2	s	67	37164.53	3	s
28	41807.78	4	s	68	37070.34	1	s
29	41732.53	4	s	69	37053.97	3	s
30	41722.13	3	s	70	36912.31	3	s
31	41652.59	3	s	71	36873.28	0	s
32	41483.33	3	s	72	36855.17	3	s
33	41465.89	3	s	73	36812.63	3	s
34	41354.57	3	s	74	36776.39	3	w
35	41259.38	3	s	75	36762.99	3	s
36	41059.11	0	w	76	36390.96	0	m
37	40525.48	2	w	77	36238.66	3	m
38	40077.22	1	w	78	36223.69	3	m
39	40071.43	4	w	79	36161.92	3	m
40	40036.70	1	w				

Turning now to Table 3, one may find a slightly different situation: unlike Table 2, the spectroscopic information shown in Table 3 confirms the previous results of both level energy and line intensity. Although in the present work different excitation schemes from the previous experiments are used,[22,29] the spectral data of the 82 states as shown in Table 3 accord well with the previous experimental results within an experimental uncertainty. However, in the present work a unique J value can be assigned to all the states, which have been assigned only with two or three possible J values previously.

Table 3. Level energy E values and relative intensity I values of Sm even-parity states, to be compared with those in Refs. [22] and [29]. The unique J assignment is also given.

Serial number	E/cm^{-1}	J	I	Serial number	E/cm^{-1}	J	I
1	42018.74	2	s	42	38591.50	3	s
2	41916.15	3	s	43	38482.21	2	w
3	41907.42	2	w	44	38166.38	4	w
4	41887.10	1	w	45	38147.34	2	w
5	41819.50	1	m	46	38128.35	2	s
6	41800.92	3	w	47	38122.01	3	w
7	41789.32	2	m	48	38114.82	4	m
8	41765.88	2	m	49	38109.20	2	m
9	41621.54	3	w	50	38083.96	2	s
10	41563.74	3	m	51	38043.77	3	m
11	41286.47	3	w	52	38035.39	3	m
12	40791.08	1	m	53	38024.85	1	w
13	40761.14	2	m	54	37998.39	3	m
14	40724.56	2	w	55	37971.10	2	m
15	40687.18	2	w	56	37967.64	1	s
16	40616.48	2	w	57	37943.61	1	s
17	40086.30	1	w	58	37922.22	3	w
18	39961.50	1	w	59	37899.31	3	s
19	39673.43	1	s	60	37877.84	4	w
20	39626.58	1	s	61	37812.13	1	m
21	39439.55	4	s	62	37771.88	4	m
22	39272.12	3	w	63	37762.19	4	m
23	39339.09	3	s	64	37708.09	1	s
24	39153.92	3	m	65	37679.41	1	m
25	39105.92	2	w	66	37576.46	2	s
26	39095.58	3	m	67	37568.45	3	s
27	38910.26	2	s	68	37561.07	1	w
28	38890.66	2	w	69	37493.68	1	m
29	38883.20	3	s	70	37460.68	3	m
30	38853.60	3	s	71	37453.82	2	s
31	38848.01	2	w	72	37430.18	1	m
32	38818.15	2	s	73	37416.27	1	w
33	38802.82	4	m	74	37386.49	2	s
34	38773.88	3	w	75	37342.36	3	w
35	38763.56	3	s	76	37339.68	1	s
36	38760.28	3	s	77	37259.07	3	s
37	38737.86	1	s	78	37244.19	3	s
38	38708.71	4	w	79	36996.33	3	m
39	38673.13	1	s	80	36682.16	3	m
40	38633.79	3	m	81	36409.07	3	s
41	38608.31	2	s	82	36364.01	3	m

As shown in Table 3, one may find the following facts: (a) no $J = 0$ state is found; (b) the numbers of $J = 1$, 2 and 3 states are almost the same; (c) the number of $J = 4$ states is much smaller than those with other J values.

Unlike the situation shown in Tables 2 and 3 where some new spectroscopic information is added to the published states, the present work, more importantly, also provides 109 states that have not been reported before, about which the information is shown in Table 4.

Table 4. Even-parity states yet unavailable previously. The information about their level energies, relative line intensities and a unique J assignment is given.

Serial number	E/cm^{-1}	J	I	Serial number	E/cm^{-1}	J	I
1	42249.19	4	m	56	41010.90	3	m
2	42231.94	2	s	57	40981.56	3	s
3	42205.27	0	w	58	40949.24	3	m
4	42201.20	3	m	59	40947.20	0	s
5	42168.26	3	m	60	40903.34	3	s
6	42155.80	0	w	61	40847.95	2	m
7	42149.50	4	w	62	40769.77	2	m
8	42124.91	4	s	63	40763.67	2	w
9	42090.24	1	w	64	40587.42	2	m
10	42088.00	4	m	65	40571.23	2	m
11	42081.08	0	w	66	40506.94	2	m
12	42060.29	4	m	67	40473.03	2	m
13	42009.34	4	s	68	40084.65	4	w
14	41998.65	3	s	69	39945.90	1	w
15	41963.92	4	m	70	39935.19	1	m
16	41948.61	4	m	71	39718.47	4	w
17	41883.25	4	w	72	39693.46	1	w
18	41866.59	4	m	73	39663.29	4	m
19	41856.38	4	s	74	39615.13	1	s
20	41818.08	4	m	75	39572.56	1	w
21	41816.43	0	w	76	39543.74	1	w
22	41813.62	0	w	77	39503.51	4	m
23	41812.34	4	w	78	39495.80	4	w
24	41780.38	4	m	79	39454.70	1	w
25	41775.37	3	w	80	39419.37	3	w
26	41751.95	2	m	81	39386.98	0	w
27	41737.07	3	m	82	39315.55	0	m
28	41635.65	0	w	83	39265.44	3	w
29	41613.81	3	s	84	39226.75	3	m
30	41557.36	0	w	85	39177.36	0	w
31	41550.36	3	s	86	39123.38	3	m
32	41541.01	3	m	87	38812.99	0	w
33	41518.81	3	m	88	38778.89	4	w
34	41450.18	3	s	89	38656.06	4	w
35	41433.23	0	m	90	38604.86	4	w
36	41429.38	3	s	91	37946.59	4	m
37	41427.53	0	w	92	37930.96	4	s
38	41411.53	3	w	93	37903.02	2	m
39	41405.96	3	w	94	37699.73	4	s
40	41380.50	3	s	95	37655.69	4	s
41	41301.86	0	w	96	37596.39	4	m
42	41298.62	0	m	97	37587.75	3	m
43	41277.90	3	s	98	37572.46	4	m
44	41219.75	3	s	99	37472.42	4	w
45	41216.32	3	s	100	37444.07	3	m
46	41206.65	0	w	101	37418.10	1	w
47	41192.70	3	s	102	37401.03	4	s
48	41187.82	3	m	103	37321.18	0	w
49	41156.44	3	s	104	37129.48	3	s
50	41107.72	3	s	105	37111.93	3	m
51	41090.68	3	w	106	37093.41	0	m
52	41049.76	3	s	107	37021.74	0	w
53	41048.22	0	w	108	36889.99	3	s
54	41034.01	3	s	109	36307.61	0	s
55	41013.11	0	w				

As shown in Table 4, not only their level energies and relative line intensities are determined, but also a unique J assignment is given to all the states. On the other hand, since the different excitation schemes from those references are empolyed, the number of the $J = 0$ states in Table 4 is much more than that in Table 2. As their line intensities are weak in most cases, it may be the possible reason that the number of $J = 0$ states in those references is much less.

Although in the present work a unique J can be assigned to all the states observed, the information about other quantum numbers is difficult to obtain from the experiment alone. For instance, the possible final states excited by the λ_2 photon from the $4f^6 6s6p(^7D_J)$ states, where $J = 1, 2, 3$, can be either the Rydberg states or the valence states, where the former have the $4f^6 6snl$ ($l = 0, 2$) configurations and the latter have the $4f^5 5d6s6p$ configuration. Keeping the above information in mind, neither the n-value nor the l-assignment of the $4f^6 6sn$ Rydberg states can be determined. Namely, although one may classify the experimental peaks in terms of their energy positions, a further step towards a full assignment of one specific peak requires a significant theoretical effort. Recently, such a work was performed on the simplest rare-earth atom,[30] where the Sc atom with only three valence electrons $3d4s^2$ was treated by the relativistic multichannel theory within the framework of multichannel quantum defect theory. However, for the Sm atom with eight optically active electrons, such a theoretical analysis has not appeared so far.

Now we recall the fact that the unexpected signals mentioned in Section 2 can also be discriminated from the present experiment. The process, $\lambda_2 + \lambda_2 + \lambda_2$, is found to be highly dependent on the wavelength of λ_2. Namely, there is only such a transition in the range between 530 nm and 700 nm, while 52 transitions can be found in the range between 476 nm and 530 nm as listed in Table 5.

Table 5. Observed transitions originating from the second dye laser alone and the extra information about the relative intensities of the relevant transitions.

Serial number	λ_2/nm	I	Serial number	λ_2/nm	I	Serial number	λ_2/nm	I
1	476.026	s	19	478.965	w	37	490.629	s
2	476.096	s	20	479.024	w	38	491.045	s
3	476.175	m	21	479.314	w	39	491.120	m
4	476.273	s	22	481.765	w	40	491.197	s
5	476.420	m	23	484.526	w	41	491.228	w
6	476.564	s	24	484.915	w	42	492.268	w
7	477.163	m	25	484.954	m	43	497.314	w
8	477.388	m	26	485.574	w	44	498.027	w
9	477.445	m	27	486.088	w	45	506.244	s
10	477.517	w	28	487.473	w	46	508.839	w
11	477.847	w	29	487.602	w	47	509.018	w
12	478.151	w	30	487.792	w	48	511.695	w
13	478.264	m	31	487.978	w	49	512.543	w
14	478.333	w	32	488.318	w	50	514.724	w
15	478.485	s	33	488.495	m	51	516.304	w
16	478.719	s	34	488.515	w	52	517.286	w
17	478.726	w	35	488.523	w	53	653.648	m
18	478.741	w	36	489.813	w			

It is worth while mentioning that the Sm atom can hardly be photoionized with the λ_2 photon alone when it is longer than 585 nm, while it is not the case in the shorter-wavelength range where much more transitions of this kind can be identified. Although it is impossible to give any assignments to these transitions, they are identified as the unexpected signals from the λ_2 photon alone.

4. Conclusion

The spectra of the even-parity states of the Sm atom are systematically studied with a two-colour stepwise excitation and photoionization process. With

the three different excitation paths performed in an energy region between 36160 cm^{-1} and 42250 cm^{-1}, 270 bound even-parity states of the Sm atom are detected in the present work. Although 161 of them were reported previously, the present work confirms them by using different excitation schemes. Among the 161 states, the relative line intensities of 79 states are newly given and the remaining ambiguities of J-assignment for all 161 states are eliminated in the present work. More importantly, the additional 109 states observed in the present work have not been reported previously. Their level energies, relative line intensities and a unique J-assignment are determined with the three excitation paths. Futhermore, 53 single-colour transitions originating from the second dye laser alone are also identified. Since only the J-assignment to all states can be given in the present work, more effort is required, both experimentally and theoretically, to obtain a full assignment to them.

References

[1] Dai C J 1996 *Phys. Rev.* A **53** 3237

[2] Dou W D, Dai C J and Li S B 2004 *J. Quantat. Spectr. Radia. Trans.* **85** 145

[3] Li S B and Dai C J 2003 *J. Quantat. Spectr. Radia. Trans.* **77** 345

[4] Dai C J and Lu J 1996 *J. Phys.* B **29** 2473

[5] Ali R, Nadeem A, Yaseen M, Aslam M, Bhatti S A and Baig M A 1999 *J. Phys.* B: *At. Mol. Opt. Phys.* **32** 4361

[6] Bekov G I, Vidolova-Angelova E P, Ivanov L N, Letokhov V S and Mishin V I 1980 *Opt. Commun.* **2** 194

[7] Kachru R, Heuvell H B and Gallagher T F 1985 *Phys. Rev.* A **31** 700

[8] Tran N H, Pillet P, Kachru R and Gallagher T F 1984 *Phys. Rev.* A **29** 2640

[9] Li S B, Dai C J, Sun W and Xue P 2002 *J. Electron. Spectr. Rel. Phen.* **127** 183

[10] Jones R R, Dai C J and Gallagher T F 1990 *Phys. Rev.* A **41** 316

[11] Lindsay M D, Cai L T, Schinn G W, Dai C J and Gallagher T F 1992 *Phys. Rev.* A **45** 231

[12] Lindsay M D, Dai C J, Lyons B J, Mahon C R and Gallagher T F 1994 *Phys. Rev.* A **50** 5058

[13] Dai C J 1995 *Phys. Rev.* A **52** 4416

[14] Yaseen M, Ali R, Nadeem A, Bhatti S A and Baig M A 2002 *Eur. Phys. J.* D **20** 177

[15] Zhang H, Li Y M, Yan J and Wang J G 2005 *Phys. Rev.* A **71** 042705

[16] V N Fedoseev, V I Mishin, D S Vedeneev and A D Zuzikov 1991 *J. Phys.* B: *At. Mol. Opt. Phys.* **24** 1575

[17] Bushaw B A, Nortershauser W, Blaum K and Wendt K 2003 *Phys. Rev.* A **67** 022508

[18] Vidolova-Angelova E P and Ivanov L N 1991 *J. Phys.* B: *At. Mol. Opt. Phys.* **24** 4147

[19] Ali R, Yaseen M, Nadeem A, Bhatti S A and Baig M A 1999 *J. Phys.* B: *At. Mol. Opt. Phys.* **32** 953

[20] Yi J, Lee J and Kong H J 1995 *Phys. Rev.* A **51** 3053

[21] Jia L, Jing C Y, Zhou Z Y and Lin F C 1993 *J. Opt. Soc. Am.* B **10** 1317

[22] Zhao H Y, Dai C J and Guan F 2009 *J. Phys.* B: *At. Mol. Opt. Phys.* **42** 065001

[23] Gomonai A I and I Plekan O 2003 *J. Phys.* B: *At. Mol. Opt. Phys.* **36** 4155

[24] Hu S F, Zhang S, Mei S M, Qiu J Z and Chen X 1990 *J. Quantat. Spectr. Radia. Trans.* **43** 75

[25] Guan F, Dai C J and Zhao H Y 2008 *Chin. Phys.* B **17** 3655

[26] Jayasekharan T, Razvi M A N and Bhale G L 2000 *J. Opt. Soc. Am.* B **17** 1607

[27] Jayasekharan T, Razvi M A N and Bhale G L 1996 *J. Opt. Soc. Am.* B **13** 641

[28] Martin W C, Zalubas R and Hagan L 1978 *Atomic Energy Levels—The Rare-Earth Elements* NSRDS-NBS60 (Washington, D.C.: U.S. GPO) p. 162

[29] Qin W J, Dai C J, Xiao Y and Zhao H Y 2009 *Chin. Phys.* B **18** 3384

[30] Jia F D, Zhong Z P, Sun W, Xue P and Xu X Y 2009 *Phys. Rev.* A **79** 0325051